



Deposited via The University of Leeds.

White Rose Research Online URL for this paper:

<https://eprints.whiterose.ac.uk/id/eprint/86063/>

Version: Accepted Version

Article:

Leeson, AA, Shepherd, A, Briggs, K et al. (2015) Supraglacial lakes on the Greenland ice sheet advance inland under warming climate. *Nature Climate Change*, 5 (1). pp. 51-55. ISSN: 1758-678X

<https://doi.org/10.1038/nclimate2463>

Reuse

Items deposited in White Rose Research Online are protected by copyright, with all rights reserved unless indicated otherwise. They may be downloaded and/or printed for private study, or other acts as permitted by national copyright laws. The publisher or other rights holders may allow further reproduction and re-use of the full text version. This is indicated by the licence information on the White Rose Research Online record for the item.

Takedown

If you consider content in White Rose Research Online to be in breach of UK law, please notify us by emailing eprints@whiterose.ac.uk including the URL of the record and the reason for the withdrawal request.

Greenland's supraglacial lakes advance inland under warming climate

Leeson, A. A.^{1,2*}, Shepherd, A.¹, Briggs, K.¹, Howat, I.³, Fettweis, X.⁴, Morlighem, M.⁵, Rignot, E.⁵

* Corresponding author

[1] School of Earth and Environment, University of Leeds, Leeds, LS2 9JT

[2] Department of Geography, Durham University, Durham, DH1 3LE

[3] School of Earth Sciences and Byrd Polar Research Center, Ohio State University, Columbus, Ohio, USA

[4] University of Liège, Department of Geography, 2, Allée du 6 Août, Bat. B11, 4000 Liège, Belgium

[5] Department of Earth System Science, University of California, Irvine, 3200 Croul Hall, Irvine, CA 92697-3100

Supraglacial lakes (SGLs) form annually on the Greenland ice sheet^{1,2} and, when they drain, their discharge enhances ice sheet flow³ by lubricating the base⁴ and potentially by warming the ice⁵. Today, SGLs tend to form within the ablation zone, where enhanced lubrication is offset by efficient sub-glacial drainage^{6,7}. However, it is not clear what impact a warming climate will have on this arrangement. Here, we use an SGL initiation and growth⁸ model to show that lakes form at higher altitudes as temperatures rise, consistent with satellite observations⁹. Our simulations show that in south west Greenland, SGLs spread 103 to 110 km further inland by the year 2060 under moderate (RCP 4.5) and extreme (RCP 8.5) climate change scenarios, respectively, leading to an estimated 48 to 53% increase in the area over which they are distributed across the ice sheet as a whole. Up to half of these new lakes may be large enough to drain, potentially delivering water and heat to the ice sheet base in regions where sub-glacial drainage is inefficient. In such places, ice flow responds positively to increases in surface water delivered to the bed through enhanced basal lubrication^{4,10,11} and warming of the ice⁵, and so the inland advance of SGLs should be considered in projections of ice sheet change.

The volume of water stored in SGLs on the surface of the Greenland ice sheet is determined by the presence of depressions in the local terrain², by the amount of runoff⁸ (melt water plus rain minus refreezing in the snowpack) and by lake drainage³. It is estimated that 13% of Greenland's SGLs drain on timescales of the order of a few hours¹², often by the creation of moulins as water-filled fractures propagate through the full thickness of the ice sheet (termed hydro-fracture)¹³. SGLs act as a source of en- and sub-glacial water when they drain and afterwards, the moulin acts as a conduit allowing runoff to pass between the ice sheet surface and base^{1,3}. Satellite and ground-based observations show a correlation between the degree of runoff and the rate of ice motion^{4,6,7}, however there are known spatial and temporal variations in the magnitude and sign of this relationship. For example, near the ice sheet margin, lower annual ice speeds have been recorded in years of high melting^{6,7} but

further inland – at higher elevations – the reverse seems to be the case^{4,11}. This dichotomy can be attributed to an abundance of melt water at the margin, enabling the evolution of efficient sub-glacial drainage early in the melt season^{6,10}, and thicker ice and less water farther inland hindering the development of an efficient evacuation system^{14,15}. In addition to their impact on basal sliding, draining SGLs, and moulines which persist post-drainage, can exert a local warming as relatively warm water passes through the colder ice (termed cryo-hydrologic warming)⁵. This – by rendering the ice sheet more fluid – can potentially enable faster ice sheet flow due to internal deformation⁵. Ultimately, faster flow may result in mass loss as ice sheet thinning promotes an inland expansion of the melt zone.

In south west Greenland, the maximum elevation at which SGLs occur has migrated 53 km inland over the past 40 years, following an upwards shift in the ice sheet equilibrium line⁹ which, historically, has fallen close to (within 10 km on average) the maximum elevation of SGLs (Supplementary Table S1). This migration has accelerated over the past two decades, in response to rapid changes in regional temperature¹⁶ associated with global warming and an increase in frequency of negative North Atlantic Oscillation (NAO) indices during boreal summer (favouring warmer and drier atmospheric conditions than normal)¹⁷. To study the long-term response of SGLs to this and future climate change, we simulate their initiation and growth over the period 1971 to 2060 in the vicinity of the Russell and Leverett Glaciers (Fig. 1). Our simulations are performed using the SGL Initiation and Growth (SLInG) model⁸, a hydrological model which routes runoff over a model of the ice sheet surface, allowing water to form lakes in topographic depressions (Methods). Here we focus on a 19,441 km² section of the ice sheet situated at elevations more than 1100 m above sea level (a.s.l.), where sub-glacial drainage is expected to be inefficient^{10,15} and the impact of SGLs on ice sheet hydrology is potentially large. The SLInG model is forced with estimates of runoff derived from high resolution (25 km) regional climate model¹⁸ reanalyses (1971 to 2010) and future projections (2006 to 2100). Future simulations are performed under both moderate

and extreme climate projections characterised by Intergovernmental Panel on Climate Change Representative Concentration Pathways (RCPs) 4.5 and 8.5¹⁹, respectively.

Our model predicts that the maximum elevation at which SGLs occur has migrated 56 km inland in our study area since the 1970's (Fig. 2), in excellent agreement with an independent estimate (53 km) based on satellite observations acquired over the same region⁹. Both datasets reveal that the rate of inland migration was slow (0.5 km yr^{-1}) and steady until 1995, and that it accelerated sharply thereafter to its present rate of 3.0 km yr^{-1} – a sixfold increase. The step-change was in response to enhanced surface melting associated with a 2.2°C air temperature rise over the same period, with respect to the average before then¹⁶. The maximum SGL elevation in our past and present simulations exhibits a small (6%) bias with respect to the observations, and agreement between the two estimates is generally very good ($r^2=0.74$). During a six year period (2006 to 2012) when model simulations and satellite observations are both available, the agreement is even better. The RCP 4.5 simulation, where anthropogenic impacts on the greenhouse effect stabilise around 2100 at values analogous to a two-thirds increase in CO_2 , is in closest agreement with the observations ($r^2=0.76$, bias=2%). We interpret this as being an artefact of forcing data; the earth system model used to drive the runoff simulation over this time period does not capture recently observed unusual NAO activity, which is attributed to natural variability¹⁷. Overall, the SLInG model captures the historical trend in inland lake migration well, including the rapid upturn since 1996 during which observations are most abundant, providing confidence in the model's capacity to simulate SGL evolution.

Our simulations suggest that SGLs will continue to spread inland over the coming decades, at an intermediate rate that is faster than during the earliest period of our experiment (1971 to 1995), but slower than the rapid migration of recent decades (Fig. 2). Under RCPs 4.5 and 8.5, simulated SGLs spread inland in south west Greenland at 1.5 ± 1.0 and $1.2 \pm 1.3 \text{ km yr}^{-1}$ respectively, between 2013 and 2045 - about half the present rate. This slow-down is

attributed to a return to climatological NAO conditions in the forcing data. The relative uncertainty of both trends reflects the variability in runoff over intermediate timescales, driven by the underlying complexity in the climate system. The maximum altitude at which SGLs appear in our simulations stabilises at around 2200 m a.s.l. shortly after 2045 under both RCPs (Fig. 2). However this altitude coincides with the lateral limit of the elevation model used in our simulations, and it seems likely that this constitutes a lower limit given that runoff occurs farther inland in regional climate model projections beyond this date. We simulate that, under RCPs 4.5 and 8.5, SGLs will be found at 2191 m a.s.l. and 2221 m a.s.l., in at least five of the years between 2050 and 2060, increases of 399 m a.s.l. and 429 m a.s.l., respectively, compared to the present day (Table 1). This 103 to 110 km inland migration corresponds to a 10,537 to 11,283 km² (94 to 101%) increase in the area of ice over which SGLs are distributed (Fig. 1, Table 1).

SGLs are abundant and sparse below and above 1600 m a.s.l. in our study area, respectively (Fig. 1, Fig. 3b), following undulations in the bedrock topography, damped according to the thickness of the overlying ice². In our simulations of lake distributions, these depressions tend to appear in regions where basal slope is lower than average (60% of lakes) or where the bedrock is relatively smooth (61% of lakes) (Supplementary Table S2), though a more detailed analysis of these relationships will likely require bed elevation data of higher resolution than is currently available. Based on our SLInG model experiments – in particular the simulation of large lakes at high altitudes – it seems reasonable to suppose that SGLs will develop at, or near to, the ice divide in this sector of Greenland (around 2500 m a.s.l.) before 2100. Positive runoff is predicted at 2500 m a.s.l. in the regional climate model projections used here by 2050.

The inland migration of SGLs in south west Greenland under climate warming has broader implications for evolution of the ice sheet hydrology and flow elsewhere. To investigate, we derived an empirical relationship between the maximum elevation of SGLs and their latitude

(Methods) as a basis for extending our findings to other ice sheet sectors, assuming that the terrain, firn and runoff in other regions are similarly conducive to future lake formation. Under these assumptions, 550,000 and 570,000 km² (32 and 33%) of the ice sheet surface would be populated by lakes by 2060 under RCPs 4.5 and 8.5, respectively (Fig. 3), a 48 to 53% increase relative to the present day (372,000 km²). This extrapolation is least certain in the east and south east of the ice sheet, where maximum lake elevation and latitude show the poorest correlation (Supplementary Table S1 and Fig 3). We attribute this to the steep ice sheet terrain and runoff gradients typical of these areas, each of which present limitations to lake formation.

The rate of melting at the base of SGLs is approximately double that of the surrounding ice, due to their relatively low albedo²⁰, and so an expansion of SGL-covered area may also lead to increased melting. Based on our simulations, and extrapolating across the entire ice sheet (Methods), we estimate that increases in the population of SGLs will lead to a 0.7 to 0.8% increase in the volume of surface melting (6.61 to 8.54 Gt yr⁻¹) in Greenland – more than twice that which lakes contribute today. This is likely an upper limit as roughly half of SGLs are thought to drain at some point during the melt season¹², and so their potential impact on ice sheet mass balance through albedo changes alone is relatively modest.

Even though the processes controlling rapid lake drainage are not well understood, linear elastic fracture mechanics can be used to identify lakes which are large enough to hydro-fracture^{13,21}. When applied to SGLs which we simulate above the present day maximum elevation in 2060 in south west Greenland (Methods), we estimate based on a sensible range of sensitivity values that between 4 and 58 (4 to 51%) and 12 and 72 (8 to 50%) are large enough to hydro-fracture, thus making melt water available for basal lubrication and cryo-hydrologic warming, under RCPs 4.5 and 8.5 respectively. We use the Shreve hydraulic potential equation²² to map likely sub-glacial drainage pathways, were surface water to access the bed (Fig. 1, Methods). We find that the simulated SGLs form in locations allowing

easy access to the sub-glacial hydrological (potential) network in the event of drainage (220 m away on average). This suggests that if lakes drain at higher elevations than currently observed in coming years, the subsequent impact on basal sliding is likely to propagate downstream.

Although the Arctic region is predicted to warm by 2.2 to 8.3°C by 2100²³, simulations of Greenland ice sheet evolution have not considered the impact of changes in the distribution of SGLs which impact on the ice sheet surface albedo²⁰ and, when they drain, on ice flow through basal lubrication³ and en-glacial ice warming⁵. According to our simulations, even in a warmer climate the impact of SGLs on the area-averaged albedo of the ice sheet remains small. However, by 2060, we show that 94 to 108% more of our study area will host SGLs and become exposed to their influence on ice flow. Extending the results of our model, we estimate that 48 to 53% more of the ice sheet will be similarly affected. Ice in these inland areas has been shown to exhibit a positive dynamical response to increased runoff¹¹, in contrast to that at lower elevations, where the effects of enhanced basal ice lubrication are offset by efficient sub-glacial drainage⁶.

The latest ice sheet modelling studies suggest that between 0 and 27% of Greenland's projected contribution to global sea level (0.05 to 0.22 m²³) can be attributed to the impact of seasonal melt on ice sheet dynamics^{24,25}. However, these estimates are based on observations of melt-induced acceleration which have a narrow spatio-temporal extent⁴ and do not consider the potential effects of cryo-hydrologic warming⁵. Our study demonstrates that SGLs large enough to drain will in fact spread far into the ice sheet interior as climate warms, which suggests that projections of the ice sheet dynamical imbalance should be revised to account for the expected evolution in their distribution. Establishing the degree to which the inland spread of SGLs will affect future ice sheet motion is now a matter of considerable concern.

Methods

Simulation of SGLs. SLInG is a hydrological model which uses Manning's equation for open channel flow and Darcy's law for flow through a porous medium in order to route and pond water over a digital elevation model (DEM)⁸. The SLInG model has been shown to successfully reproduce observed SGL initiation and growth at both the seasonal and inter-annual timescales⁸. The DEM used in this study was generated using Interferometric Synthetic Aperture Radar (InSAR) data acquired in the winter of 1995/1996 by the European Remote Sensing satellites (ERS-1 and ERS-2). By comparison with IceSat altimetry measurements, the DEM is estimated to reproduce the vertical location of the ice sheet surface to within 11.8 m (root mean squared deviation) with a precision (r^2) of 1.0. The DEM extends farther inland than previous high-resolution models, and exhibits surface depressions farther inland than the current upper limit of SGL formation.

Three model experiments were performed using runoff estimates derived from version 2 of the Modèle Atmosphérique Régional (MAR) regional climate model, which includes a comprehensive snow model that explicitly accounts for the retention and refreezing of runoff.¹⁸ These comprised an experiment covering the 1971 to 2010 period (past and present) and two experiments covering the 2010 to 2100 period (future) under moderate and extreme climate scenarios characterised by RCPs 4.5 and 8.5 respectively. Global mean temperature change under RCPs 4.5 and 8.5 is projected to be 1.8°C (1.1 to 2.6°C) and 3.7°C (2.6 to 4.8°C) by 2100. MAR was forced at the boundaries by the European Centre for Medium-Range Weather Forecasts (ECMWF) ERA-40 reanalysis for simulations covering 1971 to 1989 and the ERA-Interim reanalysis for simulations covering 1990 to 2010. For future simulations, MAR was forced by the CanESM2 Earth System Model from the CMIP5 data base (used in the Intergovernmental Panel on Climate Change fifth assessment report). CanESM2 has been shown to successfully reproduce the atmospheric circulation in the Arctic²⁶.

Estimate of SGL drainage. The amount of water required to hydrofracture thick ice, is linearly related to ice thickness, where the slope of this relationship is determined by the shear modulus of the ice²¹. The shear modulus of ice depends on multiple factors which, for thick ice sheets, are imperfectly understood (e.g. strain rate, grain size, impurities, and temperature)²⁷. However, within a range of sensible values (3.9 – 0.32 GPa²⁷), SGLs are required to be larger than 0.13 km² - 0.5 km² for hydro-fracture to occur through ~1 km of ice²¹. Extrapolating this relationship forward, we estimate that in order to hydro-fracture ~2 km of ice, SGLs need to have an area greater than 0.18 km² - 2.14 km², depending on shear modulus. In our simulations, 51% and 4% of SGLs which form above the present day maximum elevation in 2060 under the RCP 4.5 scenario have an area greater than 0.18 km² and 2.14 km² respectively. Under RCP 8.5, 50% and 8% of SGLs meet these criteria.

Ice sheet-wide extrapolation. The maximum elevation at which lakes are found (z_{max}) is close to the ice sheet equilibrium line altitude (Supplementary Table S1) which, in turn, has been described as a function of latitude²⁸ (L). We follow this approach and use satellite observations of the average maximum lake elevation at 12 sites⁹ over the period 2000 to 2010 to develop an empirical model (Eq. 1, $r^2=0.9$) to describe the spatial variation in z_{max}

$$z_{max} = -51.45L + 5229 \quad (1)$$

Estimate of SGL-enhanced melting. We characterised the impact, I , of SGLs on melting by percentage additional melt with respect to bare ice. We calculate I by assuming that the melt rate ($\dot{\alpha}$) beneath SGLs is twice that of the surrounding ice and using equation (2). Total lake area (A_{lakes}) is estimated for the entire ice sheet by multiplying lake density modelled in the study region, by the total lake-covered area (including that which lies below 1100 m a.s.l.) observed in the present and simulated in the future.

$$I = 100 * \left(\frac{(\alpha_{ice} * A_{ice} + \alpha_{lakes} * A_{lakes})}{A_{total}} - \frac{\alpha_{ice} * A_{total}}{A_{total}} \right) \quad (2)$$

Sub-glacial hydrology. A hydraulic potential field was calculated using Shreve's hydraulic potential equation and DEMs of the ice surface and bed²⁹, under the assumption that the ice sheet is warm-based; equation (3).

$$\varphi = \rho_w g h + P_w \quad (3)$$

Where h is the bedrock elevation and P_w is the sub-glacial water pressure. Here we assume that the effective pressure is negligible compared to ice over-burden pressure and thus P_w can be represented by ice overburden pressure only: $\rho_i g H$ where H is ice thickness.

Spatial analysis tools in ArcMap were used to calculate the preferential flow direction of each cell in the hydrological potential field and the corresponding potential accumulation for each cell. Cells with higher than average accumulation were assumed to form a sub-glacial hydrological network. Individual catchments were identified based on their exit point at the ice sheet margin.

References

- 1 Leeson, A. A. *et al.* A comparison of supraglacial lake observations derived from MODIS imagery at the western margin of the Greenland ice sheet. *J. Glaciol.* **59**, 1179-1188 (2013).
- 2 Lampkin, D. J. & VanderBerg, J. A preliminary investigation of the influence of basal and surface topography on supraglacial lake distribution near Jakobshavn Isbrae, western Greenland. *Hydrol. Process.* **25**, 3347-3355 (2011).
- 3 Das, S. B. *et al.* Fracture propagation to the base of the Greenland Ice Sheet during supraglacial lake drainage. *Science* **320**, 778-781 (2008).
- 4 Zwally, H. J. *et al.* Surface melt-induced acceleration of Greenland ice-sheet flow. *Science* **297**, 218-222 (2002).
- 5 Phillips, T., Rajaram, H. & Steffen, K. Cryo-hydrologic warming: A potential mechanism for rapid thermal response of ice sheets. *Geophys. Res. Lett.* **37**, L20503 (2010).
- 6 Sole, A. *et al.* Winter motion mediates dynamic response of the Greenland Ice Sheet to warmer summers. *Geophys. Res. Lett.* **40**, 3940-3944 (2013).
- 7 Sundal, A. V. *et al.* Melt-induced speed-up of Greenland ice sheet offset by efficient subglacial drainage. *Nature* **469**, 522-524 (2011).
- 8 Leeson, A. A., Shepherd, A., Palmer, S., Sundal, A. & Fettweis, X. Simulating the growth of supraglacial lakes at the western margin of the Greenland ice sheet. *The Cryosphere* **6**, 1077-1086, doi:10.5194/tc-6-1077-2012 (2012).
- 9 Howat, I. M., de la Peña, S., van Angelen, J. H., Lenaerts, J. T. M. & van den Broeke, M. R. Expansion of meltwater lakes on the Greenland Ice Sheet. *The Cryosphere* **7**, 201-204, doi:10.5194/tc-7-201-2013 (2013).
- 10 Schoof, C. Ice-sheet acceleration driven by melt supply variability. *Nature* **468**, 803-806 (2010).
- 11 Doyle, S. H. *et al.* Persistent flow acceleration within the interior of the Greenland ice sheet. *Geophys. Res. Lett.* **41**, 899-905 (2014).

- 12 Selmes, N., Murray, T. & James, T. D. Characterizing supraglacial lake drainage and freezing on the Greenland Ice Sheet. *The Cryosphere Discuss.* **7**, 475-505, doi:10.5194/tcd-7-475-2013 (2013).
- 13 van der Veen, C. J. Fracture propagation as means of rapidly transferring surface meltwater to the base of glaciers. *Geophys. Res. Lett.* **34**, L01501 (2007).
- 14 Meierbachtol, T., Harper, J. & Humphrey, N. Basal Drainage System Response to Increasing Surface Melt on the Greenland Ice Sheet. *Science* **341**, 777-779 (2013).
- 15 Chandler, D. M. *et al.* Evolution of the subglacial drainage system beneath the Greenland Ice Sheet revealed by tracers. *Nature Geoscience* **6**, 195-198 (2013).
- 16 Hanna, E., Mernild, S. H., Cappelen, J. & Steffen, K. Recent warming in Greenland in a long-term instrumental (1881-2012) climatic context: I. Evaluation of surface air temperature records. *Env. Res. Lett.* **7**, 045404, doi:10.1088/1748-9326/7/4/045404 (2012).
- 17 Fettweis, X. *et al.* Important role of the mid-tropospheric atmospheric circulation in the recent surface melt increase over the Greenland ice sheet. *The Cryosphere* **7**, 241-248, doi:10.5194/tc-7-241-2013 (2013).
- 18 Fettweis, X. *et al.* Estimating the Greenland ice sheet surface mass balance contribution to future sea level rise using the regional atmospheric climate model MAR. *The Cryosphere* **7**, 469-489, doi:10.5194/tc-7-469-2013 (2013).
- 19 van Vuuren, D. P. *et al.* The representative concentration pathways: an overview. *Clim. Change* **109**, 5-31 (2011).
- 20 Tedesco, M. *et al.* Measurement and modeling of ablation of the bottom of supraglacial lakes in western Greenland. *Geophys. Res. Lett.* **39**, L02502 (2012).
- 21 Krawczynski, M. J., Behn, M. D., Das, S. B. & Joughin, I. Constraints on the lake volume required for hydro-fracture through ice sheets. *Geophys. Res. Lett.* **36**, L10501 (2009).
- 22 Shreve, R. L. Movement of water in glaciers. *J. Glaciol.* **11**, 205-214 (1972).

- 23 Church, J. A., *et al.* in *Climate Change 2013: The Physical Science Basis*. (eds Stocker T.F., *et al.* Ch. 13, 1137–1216 (IPCC, Cambridge Univ. Press, 2013).
- 24 Parizek, B. R. & Alley, R. B. Implications of increased Greenland surface melt under global-warming scenarios: Ice sheet simulations. *Quat. Sci. Rev.* **23**, 1013–1027 (2004).
- 25 Shannon, S. R. *et al.* Enhanced basal lubrication and the contribution of the Greenland ice sheet to future sea-level rise. *Proc. Natl. Acad. Sci.* **110**, 14156-14161 (2013).
- 26 Belleflamme, A., Fettweis, X., Lang, C. & Erpicum, M. Current and future atmospheric circulation at 500 hPa over Greenland simulated by the CMIP3 and CMIP5 global models. *Clim. Dyn.* **41**, 2061-2080 (2012).
- 27 Vaughan, D. G. Tidal flexure at ice shelf margins. *J. Geophys. Res. Solid Earth* **100**, 6213-6224 (1995).
- 28 Zwally, H. J. & Giovinetto, M. B. Balance mass flux and ice velocity across the equilibrium line in drainage systems of Greenland. *J. Geophys. Res. Atmos.* **106**, 33717-33728 (2001).
- 29 Morlighem, M., Rignot, E., Mouginot, J., Seroussi, H. & Larour, E. Deeply incised submarine glacial valleys beneath the Greenland ice sheet. *Nature Geosci* **7**, 418-42 (2014).

Corresponding author

Please address correspondence and requests for materials to Amber Leeson at
a.a.leeson@leeds.ac.uk.

Acknowledgments

This work was supported by the UK National Centre for Earth Observation. We also acknowledge Professor Michiel van den Broeke who supplied surface mass balance estimates produced using the RACMO model to I.H.

Author Contributions

A. L. and A. S. designed the research. A.L. wrote and developed the SLInG model and performed all simulations/analysis. K.H.B. and A.L. created the surface DEM used as input into the SLInG model. X.F. provided runoff data from MAR simulations. M.M. and E.R. provided the bedrock DEM. I.H. provided satellite observations and ELA estimates. A. L. and A. S. wrote the paper. All authors discussed the results and commented on the manuscript.

Competing Financial Interests Statement

The authors declare no competing financial interests.

Figure 1. Simulated distribution of supraglacial lakes in 2050 to 2060 under projections of climate change. Coloured shapes indicate new lakes that appear in each scenario. Black outline indicates SLInG model domain, contours indicate: lower limit of reported results (charcoal), maximum elevation of lakes (solid colours) and the elevation of the 90th percentile of lake area (dashed colours). Likely sub-glacial drainage pathways are indicated in blue, shades represent discrete catchments. Background is Moderate Resolution Imaging Spectrometer (MODIS) image, captured in September 2003.

Figure 2. Simulated and observed trends in maximum lake elevation. (a) Comparison of model output and satellite observations for the 1971-2060 period, under two climate change scenarios. A linear fit has been applied to both datasets and indicates an upwards trend in maximum lake elevation. The dash lines denote a backwards projection from the fit. (b) Histogram of decadal average lake distribution, past and present scenario considers 2000-2010, RCPs 4.5 and 8.5 consider 2050-2060.

Figure 3. Future inland migration of SGLs on the Greenland ice sheet. Maximum elevation of SGLs at present and in the future, solid lines indicate simulated/observed values, dashed lines indicate extrapolated values. Grey shading indicates SLInG model domain for experiments described here. Inset shows relationship used for extrapolation, which is based on average maximum SGL elevation, observed between 2000 and 2010⁹; mapped letters indicate location of observations.

Table 1. Simulated changes in supraglacial lake distribution. Lake covered area represents the total area over which lakes are spread, lake area represents the sum of the maximum area attained by each individual lake. Decadal values relate to lakes simulated in SLInG model grid cells in the majority of model years. The model domain is limited to the region above 1100 m a.s.l., where ice sheet dynamics are sensitive to the effects of surface melting^{10,15}; a 3213 km² region below this is already populated by lakes.

	RCP 4.5			RCP 8.5	
	2000-2010	2050-2060	Change	2050-2060	Change
Mean lake size (km ²)	0.60	0.68	0.08	0.72	0.12
Number of lakes	459	613	154	652	193
Lake area (km ²)	276	417	141	473	197
Lake covered area (km ²)	7976	18517	10537	19265	11283
Maximum elevation of lake covered area (m a.s.l.)	1677	2191	399	2221	429
Elevation of 90th percentile of lake covered area (m a.s.l.)	1534	1747	307	1958	518

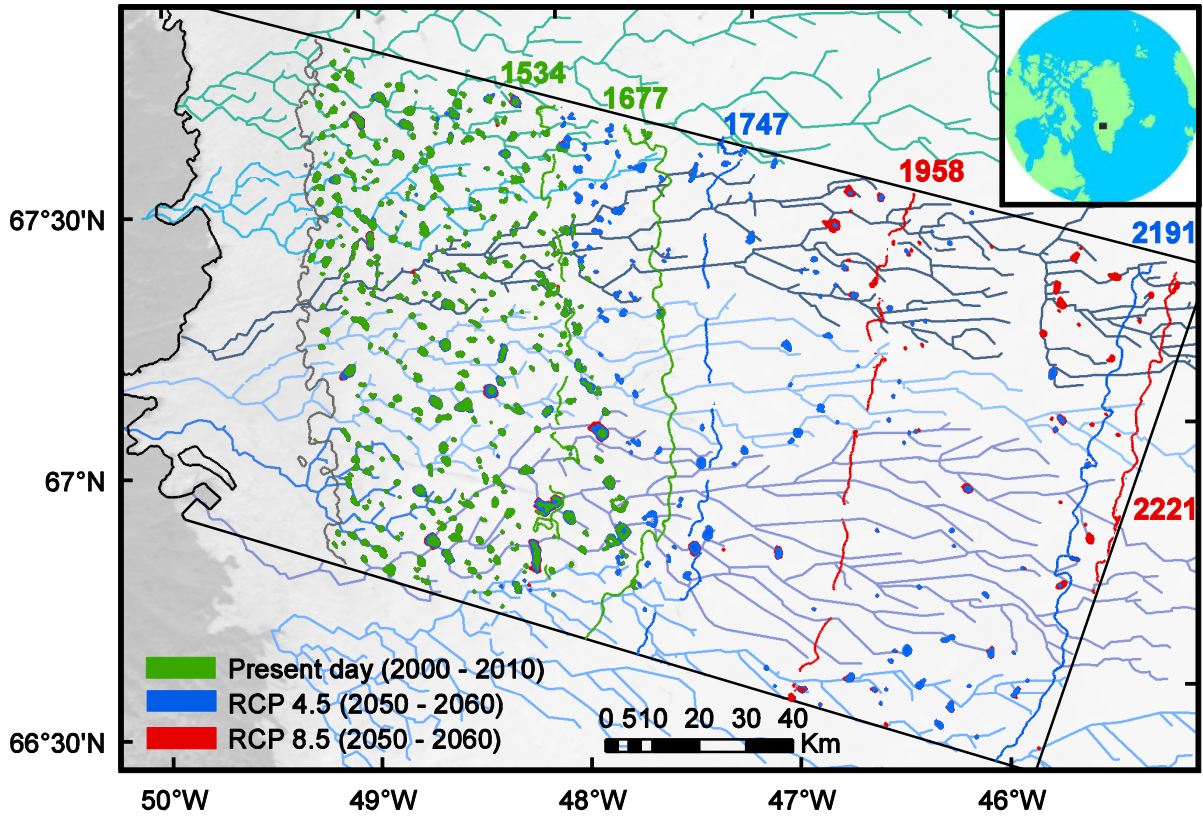


Figure 1

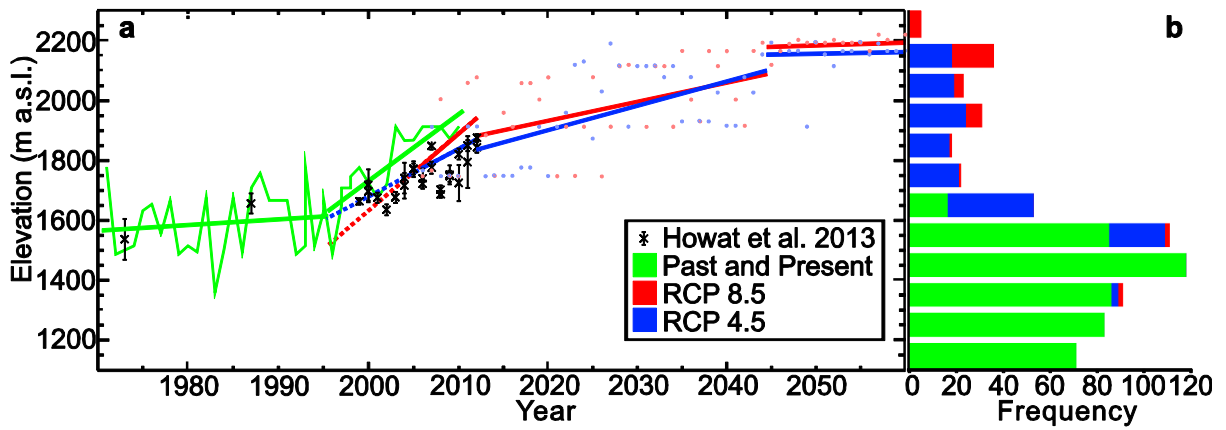


Figure 2

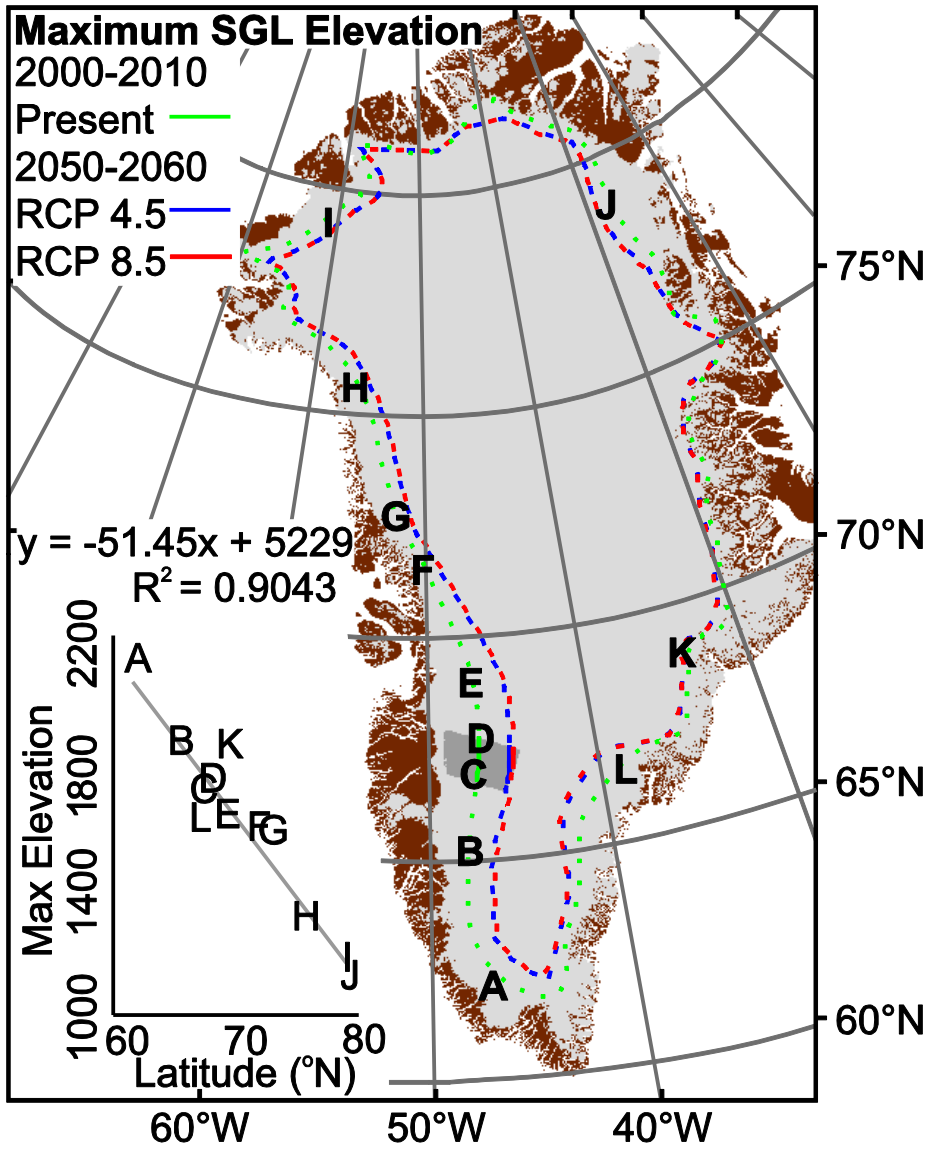


Figure 3